JOURNAL OF NEUROTRAUMA 32:1994–2007 (December 15, 2015)

DOI: 10.1089/neu.2014.3792

A Cervical Hemi-Contusion Spinal Cord Injury Model for the Investigation of Novel Therapeutics Targeting Proximal and Distal Forelimb Functional Recovery

Sarah E. Mondello,[1,2,4,*] Michael D. Sunshine,[1,*] Amanda E. Fischedick,[3,4] Chet T. Moritz,[1,2,5] and Philip J. Horner[3,4]

Abstract

Cervical spinal cord contusion is the most common human spinal cord injury, yet few rodent models replicate the pathophysiological and functional sequela of this injury. Here, we modified an electromechanical injury device and characterized the behavioral and histological changes occurring in response to a lateralized C4 contusion injury in rats. A key feature of the model includes a non-injurious touch phase where the spinal cord surface is dimpled with a consistent starting force. Animals were either left intact as a control, received a non-injury–producing touch on the surface of the cord (''sham''), or received a 0.6 mm or a 0.8 mm displacement injury. Rats were then tested on the forelimb asymmetry use test, CatWalk, and the Irvine, Beatties, and Bresnahan (IBB) cereal manipulation task to assess proximal and distal upper limb function for 12 weeks. Injuries of moderate (0.6 mm) and large (0.8 mm) displacement showed consistent differences in forelimb asymmetry, metrics of the CatWalk, and sub-scores of the IBB. Overall findings indicated long lasting proximal and distal upper limb deficits following 0.8 mm injury but transient proximal with prolonged distal limb deficits following 0.6 mm injury. Significant differences in loss of ipsilateral unmyelinated and myelinated white matter was detected between injury severities. Demyelination was primarily localized to the dorsolateral region of the hemicord and extended further rostral following 0.8 mm injury. These findings establish the C4 hemi-contusion injury as a consistent, graded model for testing novel treatments targeting forelimb functional recovery.

Key words: behavioral assessments; models of injury; spinal cord injury

Introduction

Cervical spinal cord contusion injuries (SCI) are the most prevalent type of traumatic spinal injuries causing severe deficits in arm and digit sensorimotor functions.[1,2] For individuals suffering from tetraplegia, the restoration of upper limb functions is the highest priority.[3] A well-characterized and consistent animal model of cervical SCI is imperative for accurately evaluating the efficacy of experimental therapeutics for upper limb functional recovery. Further, the discovery that spared tissue can be coaxed to form new circuits capable of bridging the injury site and restoring some function[4–6] suggests that injury models with clinically relevant tissue sparing are critical to advance therapeutic strategies. In the current study, we develop and characterize an injury model capable of producing consistent graded injuries of both proximal and distal forelimb functions while retaining substantial spared tissue capable of supporting new circuit formation for upper limb functional recovery.

At the University of Washington, we have optimized the electronics, software and mechanics of an Electromagnetic Spinal Cord Injury Device (ESCID) originally developed at The Ohio State University (OSU).[7] The current version presented here represents a fourth generation device developed over the past 14 years. Here, we characterize a rodent C4 hemi-contusion injury both behaviorally and histologically. Earlier versions of this injury device have been used to produce thoracic spinal injuries[9–12] with two exceptions: a C5 central contusion[8] and our own C4 lateral hemi-contusion.[13–15]

We sought to test the efficiency of creating graded injury severities in order to allow modeling of different potential therapeutic approaches. To accomplish this, we controlled displacement of the spinal cord in two groups: 0.6 mm or 0.8 mm. These injury magnitudes are not as severe as those previously reported, with a smaller gradation between the magnitudes tested.[8,16,17] This was done so that high levels of function would be retained in both injury groups allowing for the comparison of graded, precision-based

[1]Department of Rehabilitation Medicine, [3]Department of Neurological Surgery, [5]Department of Physiology and Biophysics, University of Washington, Seattle, Washington.
[2]The Center for Sensorimotor Neural Engineering, Seattle, Washington.
[4]The Institute for Stem Cell and Regenerative Medicine, Seattle, Washington.
*These authors are co-first authors.

deficits applicable to skilled forelimb tasks. Upper limb functional recovery was evaluated over the course of 12 weeks by assessing basic locomotor features on the CatWalk and forelimb preference on the forelimb asymmetry test. Assessments of digit dexterity and precision also were performed using the Irvine, Beatties, and Bresnahan (IBB) cereal manipulation task with a focus on comparisons of individual subscores,[18,19] which has not been utilized in prior studies characterizing cervical contusion injuries. The differences in spared tissue area, white matter, gray matter, and motoneuron counts were evaluated across the lesion epicenter and adjacent rostro-caudal regions.

All injured animals had significant behavioral deficits, compared with intact or sham operated control. The two injury severities resulted in significant differences in most behavioral measures—notably, prolonged deficits in both the proximal and distal ipsilateral upper limb following 0.8 mm injuries, while proximal upper limb function recovered quickly following 0.6 mm injuries, with only the distal upper limb deficits remaining. There were no significant differences across the two injury severities in area of spared gray matter, white matter, and lesion void at the epicenter. However, rostral extension of the lesion void and an increase in ipsilateral (un-)myelinated white matter were detected following 0.8 mm injuries but not 0.6 mm injuries. These findings establish the ESCID C4 hemi-contusion injury as capable of generating consistent and graded injuries in small groups of rats, making the device well suited for testing novel therapeutics aiming to enhance proximal and distal upper limb function by way of spared tissue-mediated circuit formation.

Methods

Subjects

All animal procedures were conducted in accordance with the National Institutes of Health guidelines for the care and use of experimental animals and were approved by the University of Washington Institutional Animal Care and Use Committee.

Updated electromagnetic spinal cord injury device

The original OSU ESCID was updated in several ways to decrease sources of variability and to allow increased flexibility for producing a variety of injury types, including thoracic, cervical, and cortical contusions.[20] Specific changes to the mechanics of the device include an update to the injury probe linkage to include a Lucite platform that is threaded directly in line with the injury probe. This provides a more rigid reference point for the non-contacting position sensor (KD-2306; Kaman Precision Products, Colorado Springs, CO), and allows for rapid modification of the reference gap when injury displacement calibration is modified between mice and rats. A threaded plate used to control the displacement has been modified to include a compression collar, which allows the displacement plate to be loosened during calibration and tightened during injuries to prevent even minor rotation of the disk (Fig. 1A).

Cervical spinal cord hemi-contusion

A total of 23 female Long Evans rats (Harlan, Indianapolis, IN) were divided into four groups: spinally intact ($n=5$), sham operated ($n=5$), 0.6 mm displacement ($n=6$), and 0.8 mm displacement ($n=7$). Animals ranged from 279-301 g at time of injury. Members of the spinally intact group did not undergo a surgical procedure, while members of the sham group received a laminectomy, as well as a non-injurious contact of the injury probe to the exposed cord to control for the laminectomy and preparatory ''touch'' that occurs before the actual injury is delivered. Members of the 0.6 mm and 0.8 mm displacement group received a laminectomy and spinal cord injury of the specified compression.

Rats were anesthetized with intraperitoneal injections of 80 mg kg^{-1} of ketamine (Pfizer, New York, NY) and 10 mg kg^{-1} of xylazine (Lloyd, Shenandoa, IA). A supplemental dose of ketamine was given if necessary. Further, rats received eye lubrication twice throughout the procedure and their hydration was maintained with Lactated Ringer's solution delivered subcutaneously (Baxter, Deerfield, IL). All surgical procedures were performed on a heated pad to maintain optimal body temperature.

An incision was made in the skin and muscle overlaying cervical segments C3-C5; muscle was then removed from the C3-C5 vertebral columns and lamina using a curette. A hemi-laminectomy was then performed on the left side of vertebral segment C4 which exposed approximately 4 mm of the spinal cord, slightly larger than the tip of the injury probe. Rats were then placed in a stereotactic frame with clamps on the spinous processes at segments C3 and C5 for stabilization during the injury procedure.

An electromagnetic probe (2 mm end diameter; Ling Dynamics, Inc., Naerum, Denmark) was oscillated in air and lowered to the surface of the exposed cord centered over the dorsal root entry zone. The probe tip was lowered into the cord until a common starting force of 4–6 kdyne was achieved for all animals (Fig. 1B, 1C). Data were sampled at 1 kHz and recorded using a USB-6229-BNC DAQ device (National Instruments Austin; TX). Subsequently, animals in the injury groups received a high-velocity injury where the spinal cord was displaced by 0.6 mm or 0.8 mm for over 14 msec (Fig. 1E). Rats in the sham group did not receive an injury. Following this, all animals were removed from the spinal frame and their exposed spinal cord was packed with gel-foam followed by closure of muscle in three layers and the skin.

All rats were immediately moved to a post-operative heating pad where they received warmed Lactated Ringer's solution (Baxter, Deerfield, Il) as well as buprenorphine subcutaneously (0.05 mg kg^{-1}). Rats continued to receive buprenorphine twice daily for 2 d.

Behavioral tasks and training paradigm

Several weeks before rats received their spinal cord injuries they were trained to comfortably walk across a CatWalk (Noldus, Leesburg, VA),[21] as well as perform a forelimb asymmetry use task[22] and cereal manipulation task.[18] These tasks were specifically chosen in order to measure motor functions ranging from basic locomotion to precise digit manipulation. Once rats were proficient at completing these tasks, they were filmed doing so for pre-injury data collection.

IBB cereal manipulation task

The cereal manipulation task, also known as the IBB[18] was used to measure changes to proximal forelimb and fine digit manipulation once per week after injury over the course of a 12-week recovery period. Animals were placed in a clear acrylic cylinder and given both donut shaped cereal (Froot Loops; Kellogg's, Battle Creek, MI) and spherical shaped cereal (Reese's Puffs; General Mills, Minneapolis, MN). They were filmed as they picked up and manipulated each piece of cereal for consumption (two pieces total) focusing on the left, ipsilateral to injury, forelimb. For scoring purposes, an individual blinded to the injury groups watched the video footage at 40% of normal speed and checked off specific functional features of the left forelimb using the published 9-point scale.[18]

The scores for each week were then averaged across all animals within a group and compared across other groups and post-injury time-points. Sub-scores also were compared across groups by converting each qualitative sub-score to a value as follows: completely unable to achieve normalcy (aberrant) = 0; partially able to

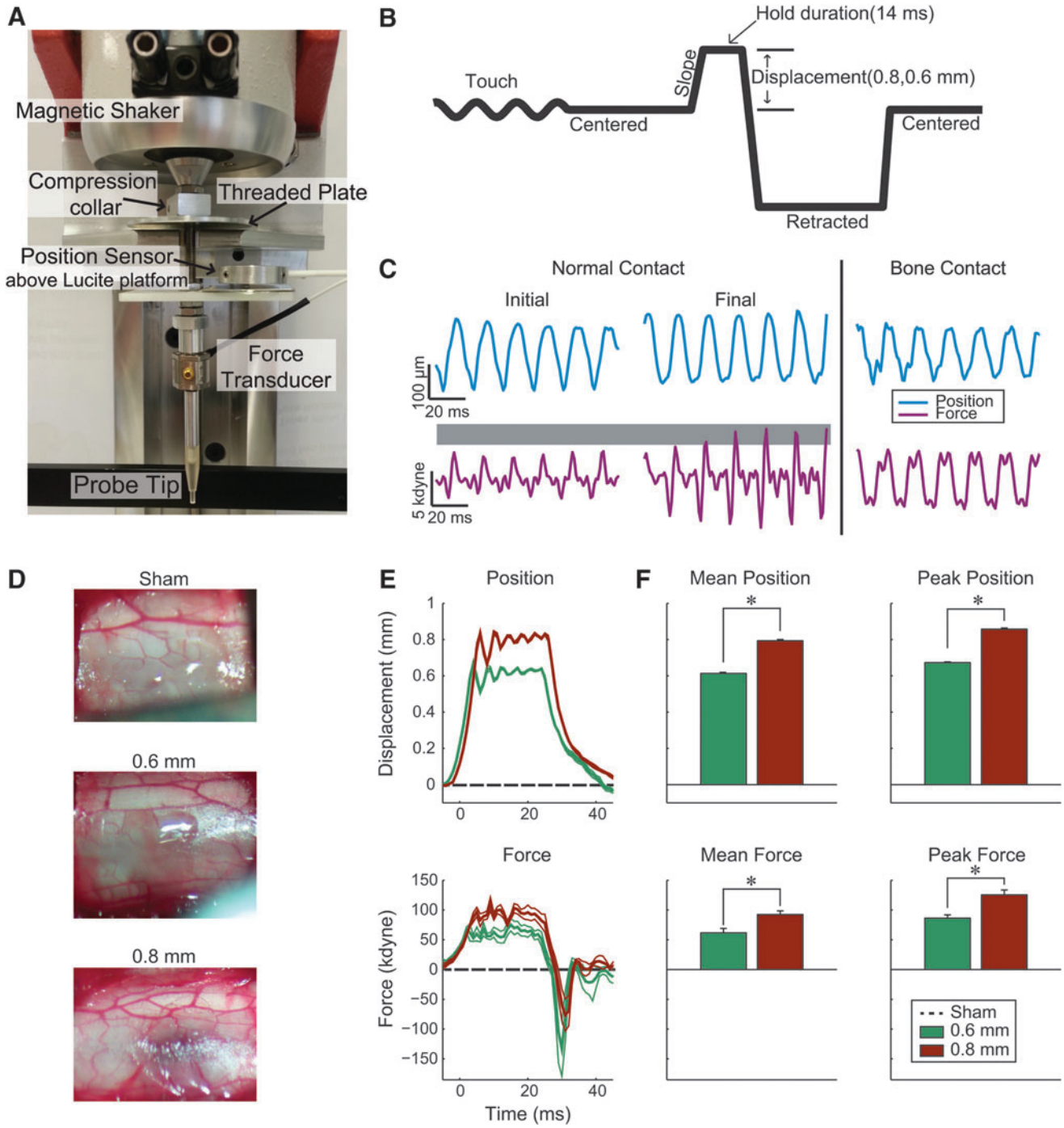

FIG. 1. Cervical contusion injury device. **(A)** Image of magnetic coil shaker, depth adjustment, force, and position sensors. **(B)** Schematic timeline of the control signal sent to the magnetic coil. Probe tip is oscillated to measure instantaneous force; oscillation is turned off prior to strike. Note: waveform is inverted, compared with actual travel of the probe; displacement occurs from the dorsal surface of the spinal cord toward the ventral spinal cord. **(C)** Touch oscillation is used to achieve consistent pre-strike force (shown as gray shaded region). Oscillation also can be used to detect aberrant contact with bone (right panel). **(D)** Representative images of the dorsal surface of the cord two min after injury (or after the touch signal was discontinued for the sham control group). **(E)** Average position and force trajectories (thick line) and standard error of the mean (SEM; thin lines, not visible in position trace). Dashed lines illustrate lack of force or displacement in sham animals. **(F)** Average and peak force and position for all injuries (Mean ± SEM; *denotes $p < 0.01$ between injury severities; 0.6 mm group, $n = 6$; 0.8 mm group, $n = 7$). Color image is available online at www.liebertpub.com/neu

achieve normalcy (anomalous) = 0.5; and completely able to achieve normalcy (normal) = 1. The volar and non-contact volar sub-scores were combined due to their close relation and converted to a more discrete numeric scale linearly distributed across a ranged from 0 to 1 as follows: zero was assigned for almost always volar and no non-volar contact; 0.1429 for almost always volar and some non-volar contact; 0.2857 for some volar and some non-volar contact; 0.4286 for some volar and almost always non-volar contact; 0.5714 for some volar and no non-volar contact; 0.7143 for no volar and almost always non-volar contact; 0.8571 for no volar and

some non-volar contact; and 1.000 for no volar and no non-volar contact. All sub-scores were averaged across the spherical and doughnut cereal types.

Forelimb asymmetry use task

In order to evaluate the changes in forelimb preference over the course of recovery,[22,23] animals were tested on a forelimb asymmetry use task once per week. Rats were placed in a clear, acrylic cylinder and were observed for up to 5 min, while a scorekeeper recorded the number of times rats reared up and made contact with the sides of the cylinder with either their ipsilateral, contralateral, or both forelimbs (dual-limb) for 20 contacts. The score was calculated by adding the number of independent ipsilateral contacts with half the number of dual-limb contacts and dividing by the total number of contacts. This was done to apply a handicap for dual-limb weight support. This was then averaged across all rats in each of the groups and the resulting values compared across groups.

CatWalk task

The CatWalk task was used to assess changes in basic locomotor features that focused on both proximal and distal upper limb function over the course of a 12-week recovery period. In a dark room, rats were trained to walk across an enclosed, 120 cm long glass walkway (Noldus, Leesburg, VA) with light transmitting through the glass walkway from below to illuminate the paw placement of all four paws. These paw prints were then reflected off an angled mirror and recorded by a camera that was connected to a computer. Each rat performed three crossing/day for up to 3 days/week to ensure enough crossings were collected for analyses. The CatWalk program software (Noldus, Leesburg, VA) then calculated six metrics for all four limbs of each run and each rat. For the purposes of this study we focused on the ipsilateral forelimb which exhibited the greatest motor deficits from the injury. These metrics include:

- Duty cycle: The percentage of time that an animal's limb is in the stance phase during the total time for each step cycle (i.e., stance duration/total step duration).
- Print area: The area (in pixels) of an animal's paw print.
- Swing duration: The period (in seconds) that an animal's limb is off the ground in swing.
- Swing speed: The speed (pixels/sec) at which an animal's limb moves from push off to paw strike (swing).
- Stand duration: The period (in seconds) that an animal's limb is placed on the ground in stance.
- Stride length: The distance (in pixels) between consecutive paw strikes.

Using custom Matlab software (MathWorks, Natick, MA), the above metrics were averaged across all runs for two consecutive weeks (i.e., Weeks 1 and 2, 3 and 4, 5 and 6, etc.) and then normalized to a percentage of each rat's pre-injury value. These values were then averaged across all rats/group, with the resulting averages compared across groups.

Perfusions and tissue preparation

Thirteen weeks after spinal cord injury, rats were deeply anesthetized with Beuthanasia (200 mg kg^{-1}), intraperitoneally. Fully sedated rats were immediately transcardially perfused first with ~300 mL of 0.9% saline followed by 300 mL of 4% paraformaldehyde in 0.1 M phosphate buffered saline (pH, 7.4). The cervical spinal cord was then dissected and stored in 4% paraformaldehyde at 4°C overnight. For the following 3 d, spinal cords were moved through a sucrose buffer gradient of 10%, 20%, and 30%, 24 h/buffer in 4°C. Tissue was then blocked into three different blocks with the first encompassing the lesion site and 1 mm rostral and caudal to the injury. The second and third blocks encompassed 3 mm of tissue immediately rostral and caudal to the lesion block, respectively. These blocks were frozen separately into Tissue Tek O.C.T. mounting media (Sakura, Netherlands) using liquid nitrogen and methylbutane. Each block was cut using a cryostat into 40 μm thick coronal sections that were stored free floating in phosphate buffered saline (pH, 7.4) at 4°C. The cords of one rat/group were blocked and cut longitudinally in order to get a global view of the tissue.

Tissue processing

Myelin staining. Every sixth section (240 μm) from blocks 1–3 were mounted onto subbed slides (Fisher Scientific, Pittsburgh, PA) coated with chrom-alum (Fisher Scientific) and gelatin (BD, Franklin Lakes, NJ). Slides were then fume fixed with 4 or 16% paraformaldehyde (Macron Chemicals, Center Valley, PA) to ensure tissue adherence. Sections then underwent a series of alcohol incubations for dehydration beginning with 5 min in water, followed by 5 min each in 70% ethanol, then 95% ethanol, then 100% ethanol, and completed with a xylene incubation for 10 min. Tissue was then rehydrated stepwise following the above procedure, inverted. Sections were then incubated for 10 mins in an aqueous myelin dye (Eriochrome Cyanine R; Fluka, St. Louis, MO) and differentiated for 1 min in 1% ammonium hydroxide (Fisher Scientific) after washing in water. Sections were dehydrated once again following the same stepwise ethanol gradients described above: 5 min each in 70% ethanol, 95% ethanol, 100% ethanol, and 10 min in xylene. Slides were coverslipped with Permount (Fisher Scientific) and then scanned using a high resolution whole-slide Nanozoomer scanner (Hamamatsu, Japan).

Myelin spared area and lesion void. Quantitative morphology was conducted by a blinded operator. Using custom-Matlab software (MathWorks) contours were drawn around the region of ipsilateral spared tissue (gray + white matter) and gray matter of each mounted and stained section to determine ipsilateral spared gray and white matter. In order to represent the rostro-caudal extent of the lesion voids, slices were aligned at the central canal. A value of −1 was assigned for the lesion area and value of + 1 was assigned to gray matter; white matter was assigned a value of 0 and all the slices containing a cystic void were then summed together to create a heat map of both the injury void and the spared gray matter. The maximum number of slices containing a cystic void was 14 which spread across 3.36 mm of tissue in the rostral-caudal dimension. Negative values (-1 to -14) were mapped in the yellow-red color space denoting the injury void regions spanning 1 (yellow) to 14 (red) sections. Positive values were mapped to the blue-green color space denoting spared gray matter spanning 1 (blue) to 14 (green) sections.

Quantification of myelinated and non-myelinated regions. Myelin stained sections were photographed at high resolution and imported into Matlab. Color images were converted to grayscale intensity images and the intensity was normalized. A blinded observer created electronic contours for analysis. After the gray matter and void contours were subtracted from the slice boundaries, the remaining white matter was separated into non-myelinated and myelinated regions by assigning pixels darker than the median image histogram as myelinated, and lighter tissue as non-myelinated. This analyses was performed on tissue for all animals with the tissue cut in cross-sections (N – 1 for each group).

Cresyl violet staining. Following the imaging of the sections stained with myelin dye, slides were de-coverslipped using an overnight incubation in xylene. Tissue was then rehydrated through a stepwise series of decreasing ethanols (100%, 95%, 70%) for

5 min each, then a 5 min incubation in water followed by a 10 min incubation in 1% ammonium hydroxide (Fisher Scientific), which removed the myelin stain (luxol fast blue). Sections were then briefly rinsed in water then incubated in cresyl violet stain (Sigma-Aldrich, St. Louis, MO) for 3 min. Following this step, sections were twice rinsed with water, then quickly dehydrated in a stepwise manner for 2 min each in 70% and 95% alcohol. The cresyl violet was then briefly differentiated in 250 mL of 95% alcohol containing five drops of glacial acetic acid (Fisher Scientific). Once differentiation was sufficient, sections continued through a stepwise dehydration process rinsed for 5 min each in 95% and 100% ethanol, followed by a final 10 min incubation in xylene. Slides were then coverslipped using Permount.

Motoneuron counts. The rostro-caudal spread of spared motoneurons was then determined for a total of 4.32 mm rostral and caudal from the epicenter. All cells with a diameter of ≥25 micrometers were included in the counts.[24] Individual slices were binned into groups of three on either side of epicenter to account for any gaps due to tissue loss during processing. This analysis was performed on tissue for all animals with cross-sectionally cut tissue (Total group N – 1).

Trichrome stain. A trichrome stain was performed to stain for collagen fibers indicating glial scarring. Every sixth section (240 μms) from a representative animal in each group was stained. Sections initially stained with cresyl violet were de-coverslipped via an overnight incubation in xylene. Sections were then rehydrated in decreasing ethanol percentages (100%, 95%), then cresyl violet stain was removed using a 10 min incubation in 250 mL of 95% ethanol with five drops of glacial acetic acid. Rehydration of the sections then continued to 70% ethanol followed by 5 min in water. Sections were then stained with Weigert's iron hematoxylin working solution (Sigma-Aldrich) for 10-15 min, followed by a wash with distilled water. Next, sections were stained in Beibrich scarlet-acid fuchsin solution (Sigma-Aldrich) for 10–15 min then washed with distilled water. Sections were then differentiated in phosphomolybdic-phosphotungstic acid solution (Sigma-Aldrich) for 10–15 min, then immediately transferred to aniline blue solution and stain (Sigma-Aldrich) for 5–10 min. Sections were then rinsed in water and differentiated in 1% acetic acid solution for 2–5 min. Lastly, sections were dehydrated stepwise in 70%, 95%, 100% alcohol, followed by xylene, then coverslipped using permount mounting media (Fisher Scientific).

Statistical analyses

Both Matlab (MathWorks) and SPSS software (IBM, Armonk, NY) were used for statistical tests. A Lilliefors test of normality was performed in Matlab to determine if the data were normally distributed, and this guided the use of parametric or non-parametric tests as described below. Two sample *t*-tests compared the average and peak of the position and force trajectories during the hold phase across 0.6 mm, and 0.8 mm injury displacement groups. One-way analysis of variance (ANOVA) tests compared among the different groups and if significant were followed by post hoc test with Bonferroni correction at individual post-injury time-points for the CatWalk, forelimb use asymmetry test, and the IBB task (combined sub-scores only). For comparisons of the individual sub-scores, the non-parametric Kruskal-Wallis test with Bonferroni corrections were used. Repeated measures ANOVAs also were used on the CatWalk, Forelimb use asymmetry test, and IBB (combined sub-scores) to compare the overall course of recovery within each group. The sham and intact groups were compared across all tasks and were not found to be significantly different, thus further comparisons focused on the non-surgical control group and the two injury severities. Power analyses were completed on the more variable measurements using G*Power, which confirmed sufficient power.

Results

The updated ESCID device produces consistent force and displacements during injury

A major source of variability in injury modeling is the challenge of establishing a common starting point for the injury probe. Prior to injury, a pre-contact force of the injury probe tip dimpling the spinal cord surface was established in each animal. The probe was oscillated at 60 Hz and lowered while observing a live force signal from the inline force transducer. The force wave amplitude increases as the probe dimples the dural surface until a target of 4–6 kdynes is achieved. This common starting force is dependent on the resistance of the spinal compartment and not the displacement itself (Fig. 1C). We observe a smooth, single sine wave if the probe is in contact with the spinal surface alone, while changes in the shape of the wave or evidence of mixed signals indicates the probe is contacting bone from an incomplete laminectomy or incidental contact of the linkage with muscle or the spinal frame (Fig. 1C, right). If the characteristics of the signal indicated non-spinal contact, the probe was repositioned to achieve a pure sinusoidal signal. In some cases where this could not be readily achieved, the laminectomy was re-inspected for evidence of bone protrusions at the laminectomy site and corrected by clearing the bone and re-attempting pure contact. In all cases, a pure signal was achieved before initiating a contusion injury.

After the touch phase, a high-velocity spinal contusion was initiated. The injury device was used to produce a graded discoloration of the spinal cord (Fig. 1D), as well as consistent position and force profiles for the 0.6 and 0.8 mm injury displacements. Saved probe position data indicated consistent and accurate spinal cord compression with significant separation between the groups. The 0.6 mm group received an average displacement of 0.61 ± 0.0016 mm and the 0.8 group an average displacement of 0.79 ± 0.0069 mm (Fig. 1E, 1F; $p < 0.0001$). Peak position was 0.67 ± 0.0041 mm and 0.85 ± 0.0059 mm for the 0.6 and 0.8 mm groups, respectively. Both average and peak force values were significantly different between injury severities (Figure 1E, 1F; $p < 0.009$), with average force and peak forces of 61.73 ± 7.46 kdyne and 86.28 ± 5.60 kdynes for the 0.6 mm group, and 91.38 ± 6.14 and 125.37 ± 8.27 kdynes for the 0.8 mm group.

IBB task

Prior to injury, rats utilized a defined set of fine digit manipulations to pick up and eat either a spherical or doughnut shaped piece of cereal.[18] Following a cervical hemi-contusion of either 0.6 or 0.8 mm displacement, this ability was significantly reduced, compared with control animals, for both the spherical shaped cereal (Fig. 2A; repeated measures ANOVA; 0.6 mm, $p < 0.0001$; 0.8 mm, $p < 0.0001$) and doughnut shaped cereal (Fig. 2B; repeated measures ANOVA; 0.6 mm, $p < 0.0001$; 0.8 mm, $p < 0.0001$). Specifically, at one week post-injury, scores on the spherical cereal fell from 9 ± 0 to 1.16 ± 0.48, and 0.86 ± 0.55 for the 0.6 and 0.8 mm groups, respectively. Similarly, scores for the doughnut shaped cereal decreased from 9 ± 0 to 1.17 ± 0.48 and 0.86 ± 0.55 for the two injury groups, respectively (Fig. 2A, 2B). Although there was some recovery over the course of 12 weeks, these scores remained significantly decreased, compared with control, in the spherical cereal (Fig. 2A; one-way ANOVA; 0.6, $p < 0.0001$; 0.8, $p < 0.0001$) and doughnut cereal (Fig. 2B; repeated measures ANOVA; 0.6, $p < 0.0001$; 0.8, $p < 0.0001$). Interestingly, animals that received a 0.6 mm injury performed significantly better than animals with a

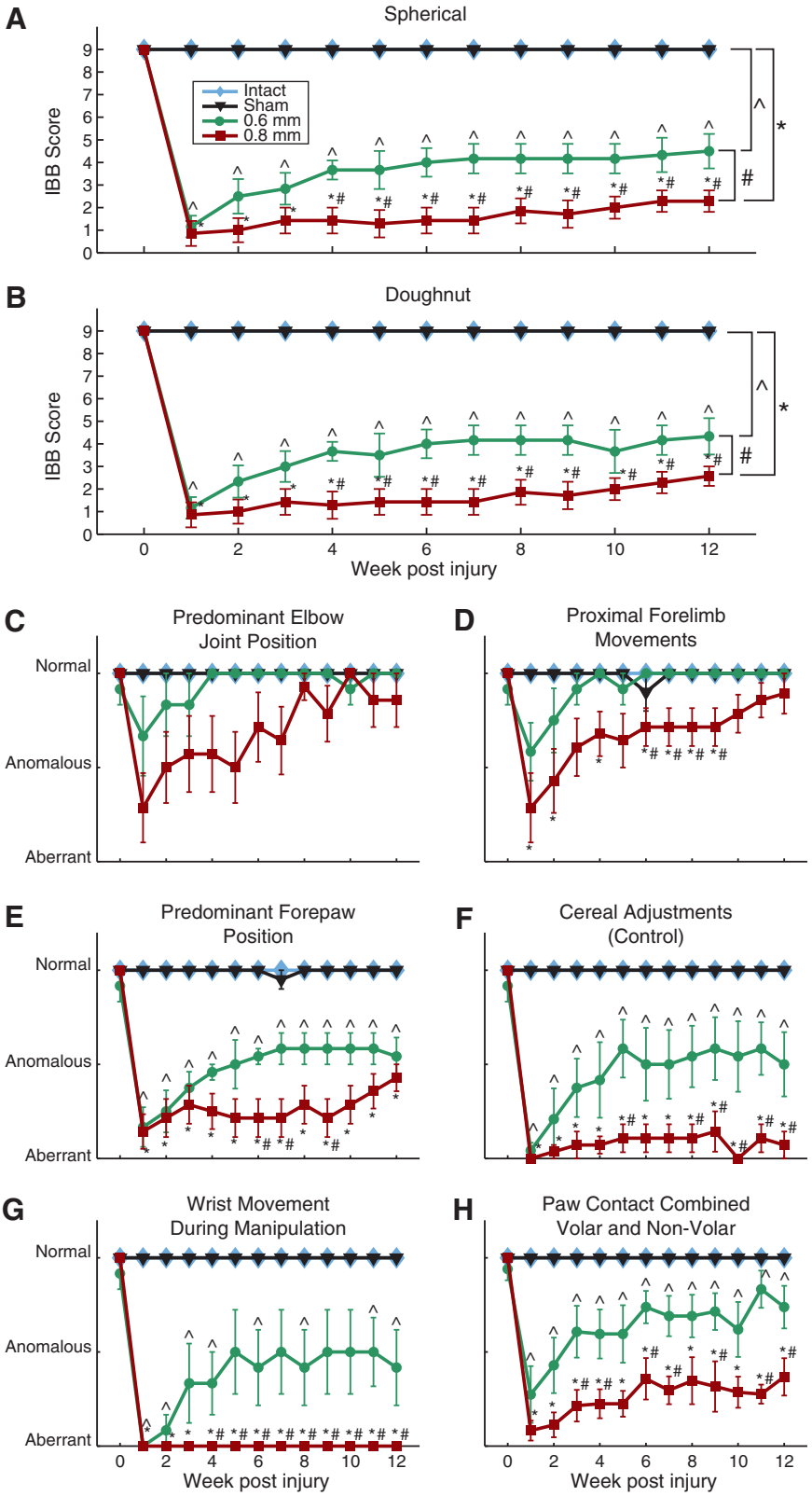

FIG. 2. Cereal manipulation task of Irvine, Beatties, and Bresnahan (IBB). Group scores for **(A)** spherical and **(B)** doughnut cereal manipulation task measured on a scale of 0-9. Cereal manipulation sub-measures for **(C)** predominant elbow joint position, **(D)** proximal forelimb movements, **(E)** predominant forepaw position, **(F)** cereal adjustments (control), **(G)** wrist movement during manipulation, and **(H)** paw contact combined volar and non-volar. Week 0 indicates pre-injury time-point. Mean ± standard error of the mean, *, ^, # denotes $p < 0.05$ for group comparison using repeated measure analysis of variance and *t*-tests. All groups are compared with the intact group ($n = 5$). Additionally, 0.6 mm injury displacement ($n = 6$) and 0.8 mm displacement ($n = 8$) are compared with one another. Color image is available online at www.liebertpub.com/neu

0.8 mm displacement injury in the spherical (Fig. 2A; repeated measures ANOVA; $p = 0.01$) and doughnut shaped cereal (Fig. 2B; repeated measures ANOVA; $p = 0.02$). This indicates a behavioral separation between these two injury magnitudes.

Assessment of the more proximal joint sub-scores (predominant elbow joint position and proximal forelimb movements) indicate that the 0.6 mm displacement group experienced minor deficits for the first three weeks after injury but recovered to control levels by the fourth week (Fig. 2C, 2D). This is in contrast to the 0.8 mm displacement group, which had significantly more aberrant functions, compared with both the control group at seven of the 12 post-injury time-points (Fig. 2D; Kruskal-Wallis, $p < 0.047$) and 0.6 mm displacement group at four of the 12 post-injury time-points (Figure 2D; Kruskal-Wallis, $p < 0.035$).

While the 0.6 mm group had minor proximal forelimb deficits, they exhibited prolonged distal forelimb deficits. Predominant forepaw position was significantly different from control in the 0.6 mm group at every time-point post-injury (Fig. 2E; Kruskal-Wallis, $p < 0.011$) and 0.8 mm group (Fig. 2E, Kruskal-Wallis, $p \leq 0.003$). The same pattern was observed for the cereal adjustments subscore in the 0.6 mm group (Fig. 2F; Kruskal-Wallis, $p < 0.034$) and 0.8 mm displacement group (Fig. 2F; Kruskal-Wallis $p \leq 0.002$). Every post-injury time-point also was significantly different from control in the contact combined volar and non-volar sub-score for the 0.6 mm (Fig. 2H, Kruskal-Wallis, $p < 0.034$) and 0.8 mm displacement groups (Fig. 2H, Kruskal-Wallis, $p < 0.009$). Additionally, the 0.6 mm and 0.8 mm groups differed from one another, with the 0.6 mm group having significantly better function than the 0.8 mm group at several different time-points for each of the above-described sub-scores (Fig. 2E, 2F, 2H; Kruskal-Wallis, $p = 0.025$, $p < 0.042$, $p < 0.043$, respectively). For the other distal forelimb sub-score, wrist movement during manipulation, the 0.6 mm group differed significantly from control at eight of the 12 post-injury time-points (Fig. 2G; Kruskal-Wallis, $p < 0.033$), while the 0.8 mm group exhibited significant deficits, compared with control, at all of the post-injury time-points (Fig. 2G; Kruskal-Wallis, $p = 0.001$). Notably, for the majority of time-points after injury, the 0.8 mm group also performed significantly worse than the 0.6 mm group, suggesting behavioral separation across the different contusion magnitudes (Fig. 2G; Kruskal-Wallis, $p < 0.042$).

Forelimb use asymmetry task

Uninjured animals lack a limb preference, using both paws equally (50%) when rearing up and exploring the cylinder (Fig. 3). Similar to reports from prior publications,[16,23] we found that spinal hemi-contusions led to a significant decrease in ipsilateral forelimb usage, compared with control animals, regardless of whether they received a 0.6 mm injury (Fig. 3; repeated measures ANOVA, $p = 0.003$) or a 0.8 mm injury (Fig. 3; repeated measures ANOVA, $p < 0.0001$). Specifically, at one week post-injury the percentage of times a rat used its ipsilateral forelimb drastically decreased from $46\% \pm 5$ to $0\% \pm 0$ in the 0.8 mm group and to $7\% \pm 7$ in the 0.6 group, which is significantly less than control (Fig. 3; one-way ANOVA, $p < 0.0001$). This significant drop in the ipsilateral forelimb was retained at most time-points for the remainder of the 12-week study period for the 0.8 mm group (Fig. 3; one-way ANOVA, $p < 0.0001$). Despite the continued reduction in ipsilateral forelimb usage compared with control, there was of some recovery over time as forelimb usage significantly increased to $16\% \pm 3$ (from 0%) in the 0.8 mm group (Fig. 3; Kruskal-Wallis, $p = 0.0012$). The 0.6 mm displacement group trended towards better performance than the 0.8 mm group with ipsilateral forelimb touches reaching $25\% \pm 7$ (from 7%) by the 12th and final week of the study. This also was a significant improvement, compared with their ipsilateral forelimb usage, at one week post-injury (Fig. 3; Kruskal-Wallis, $p = 0.045$) Notably, although the 0.6 mm displacement group reached a plateau at eight weeks post-injury, the 0.8 mm displacement group continued to show improvements at the 12 weeks post-injury

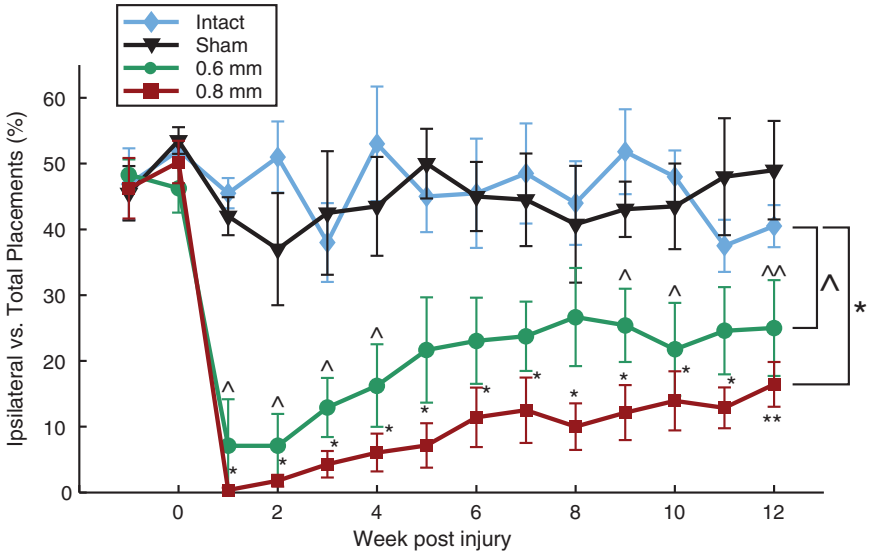

FIG. 3. Forelimb asymmetry use test. Cylinder exploration task weighted contact (independent ipsilateral contact = 1; combined contact = 0.5). Weeks -1 and 0 represent test data prior to injury (mean ± standard error of the mean). *, ^ denotes $p < 0.05$ for group comparison using repeated measure analysis of variance, all groups compared with intact ($n = 5$). Additionally, 0.6 mm ($n = 6$) and 0.8 mm injury displacement ($n = 7$) are compared with one another; **, ^^ denote $p < 0.05$ rank sum test, Week 1 post-injury, compared with Week 12 post-injury. Color image is available online at www.liebertpub.com/neu

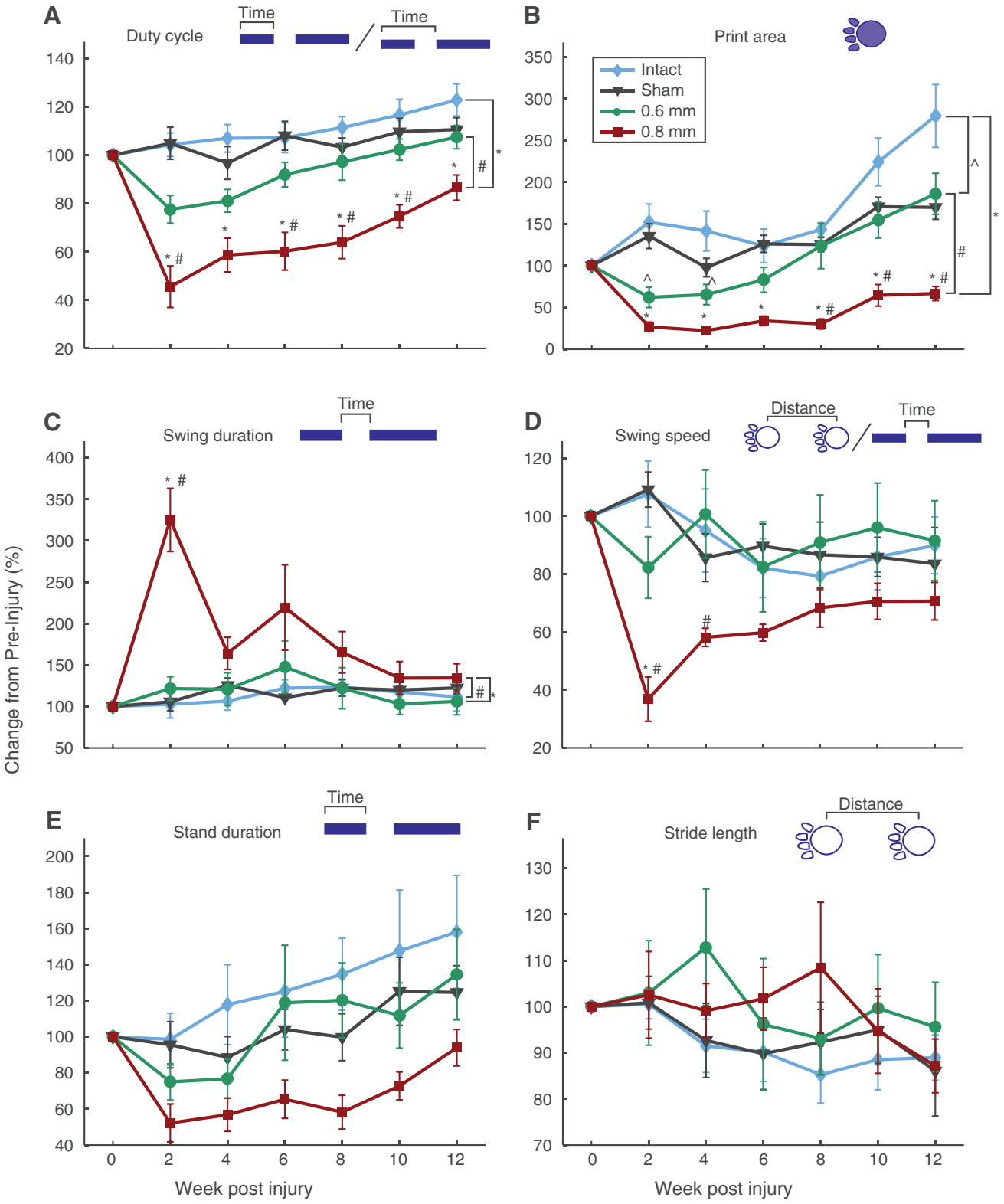

FIG. 4. CatWalk results for forelimb ipsilateral to injury. Images above each panel illustrate metric plotted below as follows: **(A)** duty cycle, **(B)** print area, **(C)** swing duration, **(D)** swing speed, **(E)** stand duration, and **(F)** stride length. Data averaged across two weeks and normalized to pre-injury (mean ± standard error of the mean) *, ^, # denotes $p < 0.05$ for group comparison using repeated measure analysis of variance. All groups compared with intact ($n = 5$). Additionally, 0.6 mm injury displacement ($n = 6$) and 0.8 mm displacement ($n = 7$) are compared with one another. Color image is available online at www.liebertpub.com/neu

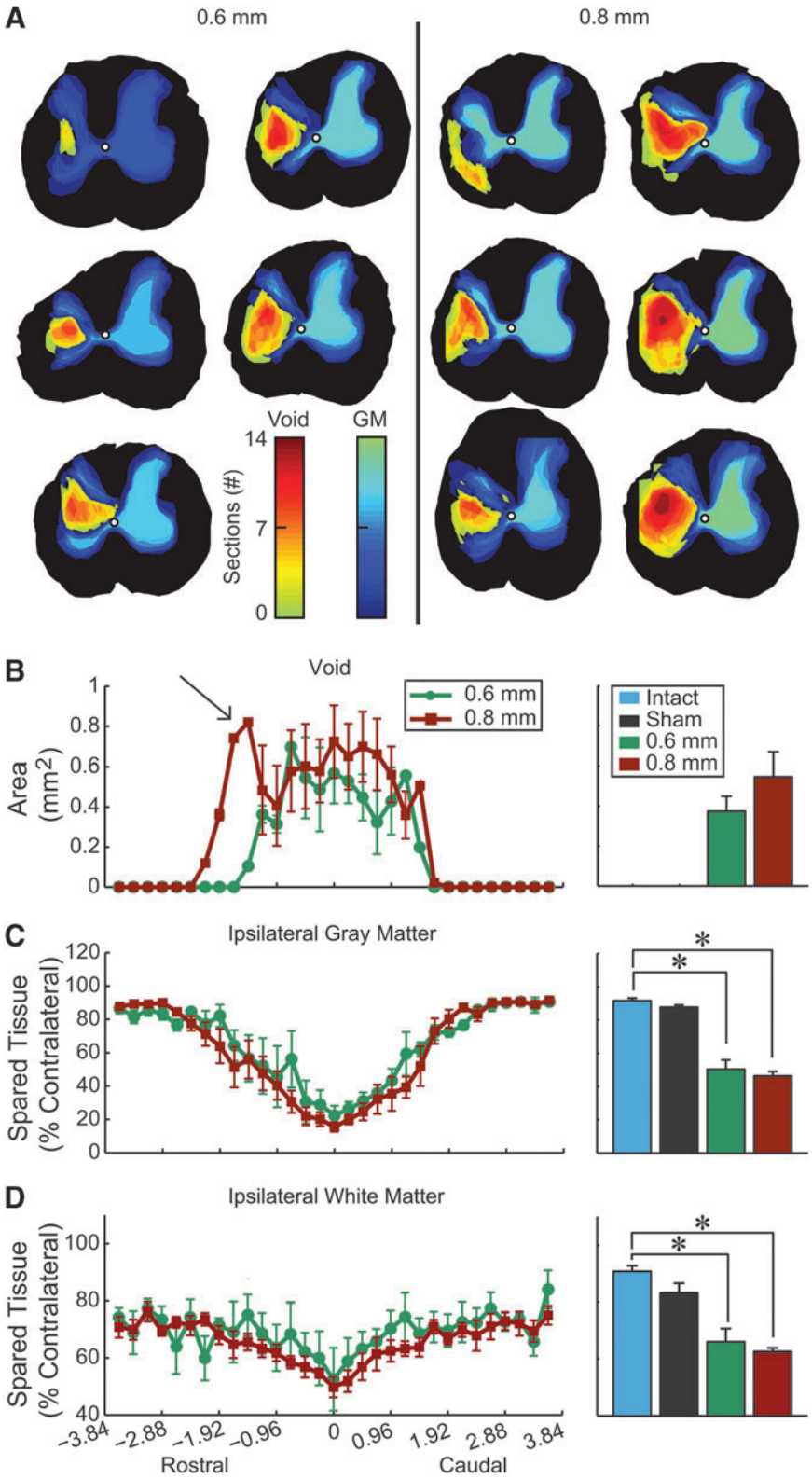

FIG. 5. Histological analysis of spared tissue. **(A)** Heat maps showing the void (yellow-red) and gray matter (green-blue) for all animals sliced in the coronal plane. Color denotes injury extent in the rostro-caudal dimension, and animals are arranged by injury void area. Rostral-caudal extent of **(B)** void area per slice, **(C)** ipsilateral gray matter sparing, and **(D)** ipsilateral white matter sparing. Arrow in B highlights greater rostral void following 0.8 mm injury. All data are normalized to the slice with the largest area on the contralateral side, except for the void volume (mean ± standard error of the mean). Bar graphs summarize the average value of each measure for tissue from the epicenter ± 2.4 mm (mean ± standard error of the mean; * denotes $p < 0.05$; intact, $n = 4$; sham, $n = 4$; 0.6 mm $n = 5$; 0.8 mm, $n = 6$). Color image is available online at www.liebertpub.com/neu

time-point. Overall, there were no significant differences between the 0.6 mm and 0.8 mm groups (Fig. 3; repeated measures ANOVA, $p = 0.597$).

CatWalk task

The CatWalk task assesses multiple locomotion-based metrics during walking across a flat, even surface. Injury severity produced differences between the 0.6, 0.8 mm, and intact groups. Duty cycle, print area, and swing duration of the 0.8 mm displacement group were significantly different from the control groups (Fig. 4A-C; repeated measures ANOVA, $p < 0.001$, $p < 0.001$, $p = 0.013$, respectively), with duty cycle, print area, and swing duration also significantly differing between the 0.6 and 0.8 mm displacement groups (Fig. 4A, 4B, 4C; repeated measures ANOVA, $p = 0.002$, 0.017, 0.002, respectively) indicating a behavioral separation across lesion magnitudes. Further, the 0.6 mm displacement group did not significantly differ from control on any of the metrics tested except for print area (Figure 4B; repeated measures ANOVA, $p = 0.011$). In the print area metric, the 0.6 mm group differed significantly from the 0.8 mm group by eight weeks post-injury (Fig. 4B; one-way ANOVA, $p = 0.001$), and this difference was maintained for the remainder of the 12-week recovery period. There were no significant differences in stand duration and stride length between the intact group and either of the injury groups (Fig. 4E, 4F). Although swing speed was initially different from the intact group in the 0.8 mm group (Fig. 4D; one-way ANOVA, $p = 0.009$), this difference disappeared lost by four weeks post-injury.

Spared tissue and lesion void

Representation of the rostro-caudal extent of the injury void and gray matter sparing for each animal in the injury groups illustrate that animals who received the larger 0.8 mm spinal displacement tended to have voids (cysts) spanning more sections than those of the 0.6 mm group (Fig. 5A). This is supported by quantified void data showing that, even though there were no significant differences in overall void area across the different displacement groups, there was an extension of the 0.8 mm displacement group in the rostral direction (arrow in Fig. 5B). While there was significantly less ipsilateral gray and white matter, compared with intact rats in the 0.6 mm group disappeared and 0.8 mm group (Fig. 5C, 5D; *t*-test, $p < 0.001$), there were no significant differences between the two displacement groups.

Ipsilateral non-myelinated white matter area was significantly greater in the 0.8 mm group, compared with 0.6 mm group (Fig. 6A; *t*-test, $p = 0.03$) with increased demyelination extending rostrally in the 0.8 mm group (Fig. 6A), paralleling results observed for the lesion void. Ipsilateral myelinated white matter also significantly differed between the 0.8 mm and 0.6 mm groups (Fig. 6B; *t*-test, $p = 0.029$) but there were no differences in rostrocaudal expression.

More detailed investigations regarding myelination of specific regions of the ipsilateral hemi-cord were completed in order to gain a greater understanding of the tract systems underlying the functional deficits seen after a 0.6 and 0.8 mm displacement hemicontusion. There were no significant group differences in the dorsal region containing the corticospinal tract (Fig. 6C), or the ventral regions containing the reticulo- and vestibulo-spinal tracts (Fig. 6E). However, the 0.8 mm group had significantly less myelination in the lateral region containing the rubrospinal tract (RST; Figure 6D; *t*-test, $p = 0.026$).

Motoneuron counts

We used a direct count of motoneurons in stained sections. While these counts can be used as an unbiased comparator between groups, we acknowledge that to quantify total motoneuron number would require the optical fractionator method we have used previously. While there was a substantial decrease in number of ipsilateral healthy motoneurons of both injury groups, compared with

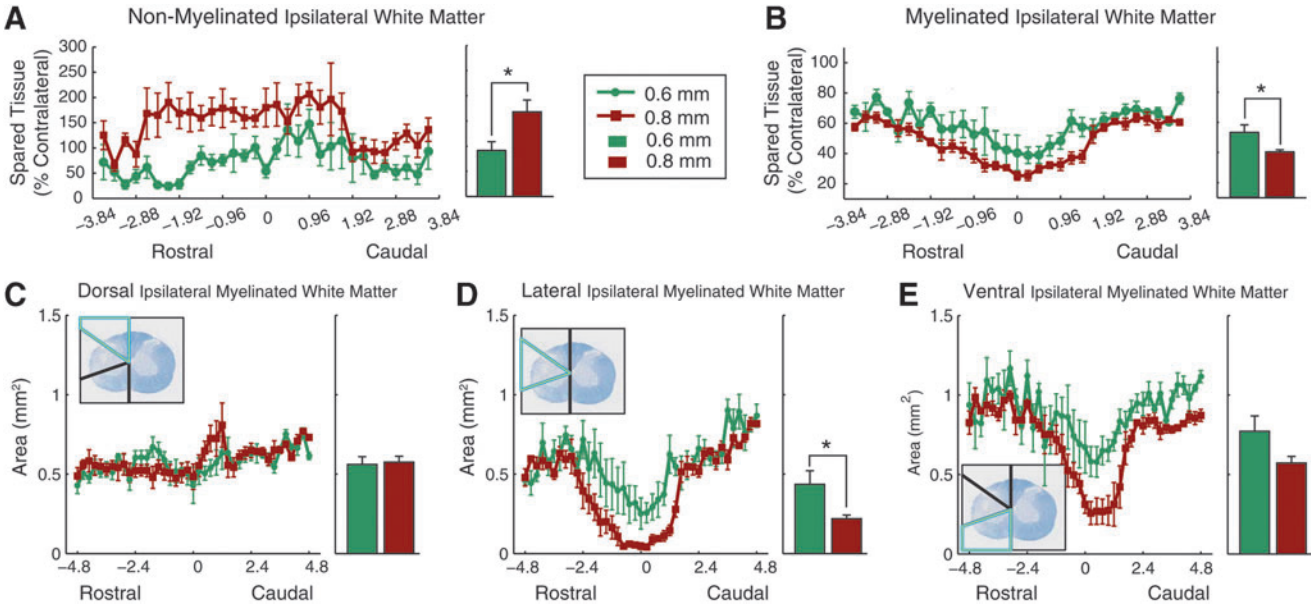

FIG. 6. Spared white matter. Spared white matter was summarized as **(A)** non-myelinated and **(B)** myelinated. Area-specific myelination within the **(C)** dorsal, **(D)** lateral, and **(E)** ventral segments of the ipsilateral side of the cord. Inset depicts region of interest (blue bounds) over an example slice from an injured (0.8 mm) animal 2.4 mm from epicenter. Bar graphs show epicenter ± 2.4 mm (mean ± standard error of the mean, * denotes $p < 0.05$; 0.6 mm $n = 5$, 0.8 mm $n = 6$). Color image is available online at www.liebertpub.com/neu

control, there were no differences between the two injury groups. In both groups, a decreased number of healthy motoneurons was detected between 2.16 mm rostral and caudal to the epicenter (Fig. 7A). Average number of motoneurons/section of both injury groups was substantially less than control groups but there were no differences in motoneuron counts between injury groups (Fig. 7B). These data indicate a relatively circumscribed injury epicenter whereby gray matter is destroyed completely within the impact zone. Gray matter at C4 is primarily lost whereas significant gray matter sparing is apparent within segments rostral and caudal (Fig. 7B).

Glial scarring

Trichrome staining was performed to assess glial scarring in representative animals from the 0.6 and 0.8 mm group. Animals with a 0.6 mm injury had more connective tissue indicating a more developed glial scar than those with a 0.8 mm injury (Fig. 8A, 8C). This was especially true in the ipsilateral ventral white matter region where the 0.8 mm animals had less connective tissue, but more small cystic regions (Fig. 8B, 8D). The latter likely indicates more extensive fiber degeneration in the 0.8 mm injury.

Discussion

Summary

We report that the updated ESCID produces consistent cervical hemi-contusions that can be graded to produce significantly different degrees of pathology and behavioral deficit. We show that following the more severe 0.8 mm injury, animals exhibit long-term proximal and severe distal forelimb deficits, while the 0.6 mm injury group exhibits transient proximal forelimb deficits but prominent distal forelimb deficits that persist for the duration of the study. These changes could be statistically resolved in small numbers of animals per group (e.g., $n=6$). Histological analyses indicate that while there were no significant differences in ipsilateral spared white matter, gray matter, or lesion void area across injury groups, the 0.8 mm group had significantly less ipsilateral myelination and demyelinated white matter. This significant lack of myelination was found to be primarily located in the lateral regions of the hemi-cord containing the dorsolateral funiculi.

The updated ESCID produces consistent, graded cervical hemi-contusion injuries. A useful SCI model requires consistency across animals in order to both reduce sample size but also increase statistical power for detecting differences in outcome. The C4 hemi-contusion model characterized in the current study displays both consistency, as well as the capability of extending this consistency across graded lesion magnitudes. Both position and force values for the two contusion magnitudes characterized in the current study were not only significantly different but also depicted markedly low variability. These findings are similar to those reported in prior studies characterizing contusion lesions of the thoracic spinal cord with earlier versions of the ESCID.[8,10,12,25] Further, we see that consistency in physical parameters of the injury probe position and sensed force translates into tight behavioral groups. Titrating the injury displacement leads to significant separation of histology and function between moderate and large injuries. This may permit assessment of potential therapeutics across a range of lesion magnitudes and associated differences in recovery timelines of sensorimotor deficits.

Distal forelimb motor function exhibits the greatest and most prolonged deficits after hemi-contusion

The CatWalk and IBB tasks showed the greatest separation between the two injury groups, identifying them as sensitive measures of this C4 cervical contusion model. Specific metrics requiring proximal forelimb functions exhibited more severe and prolonged deficits in the 0.8 mm group, compared with the 0.6 mm

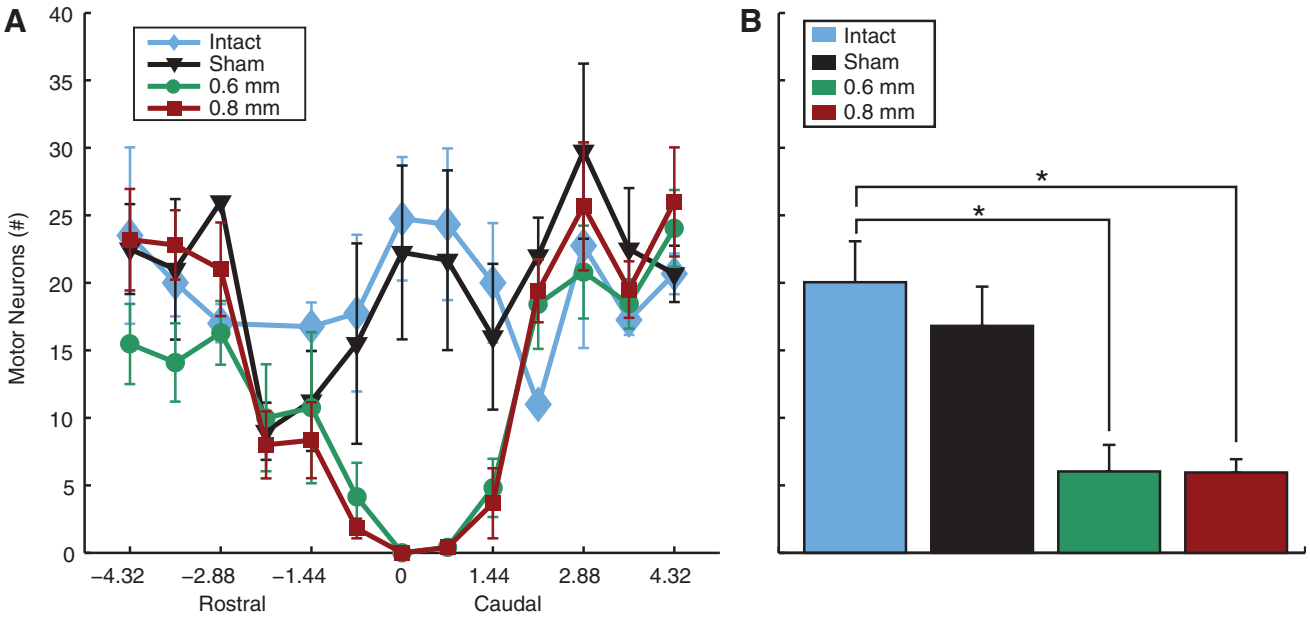

FIG. 7. Motor neuron sparing. Motor neuron sparing was estimated by counting the total number of neurons per section with a diameter greater than 25 micrometers. Quantification of cresyl violet stained sections within the hemicord ipsilateral to injury **(A)** Rostrocaudal extent of spared motoneurons over the range of 4.32 mm rostral and caudal to the lesion epicenter (Mean ± standard error of the mean). **(B)** Bar graphs of the average number of motoneurons within 2.16 mm of the injury epicenter for each group of animals (mean + standard error of the mean, * denotes $p<0.005$; intact $n=4$; sham $n=4$; 0.6 mm $n=5$; 0.8 mm $n=6$). Color image is available online at www.liebertpub.com/neu

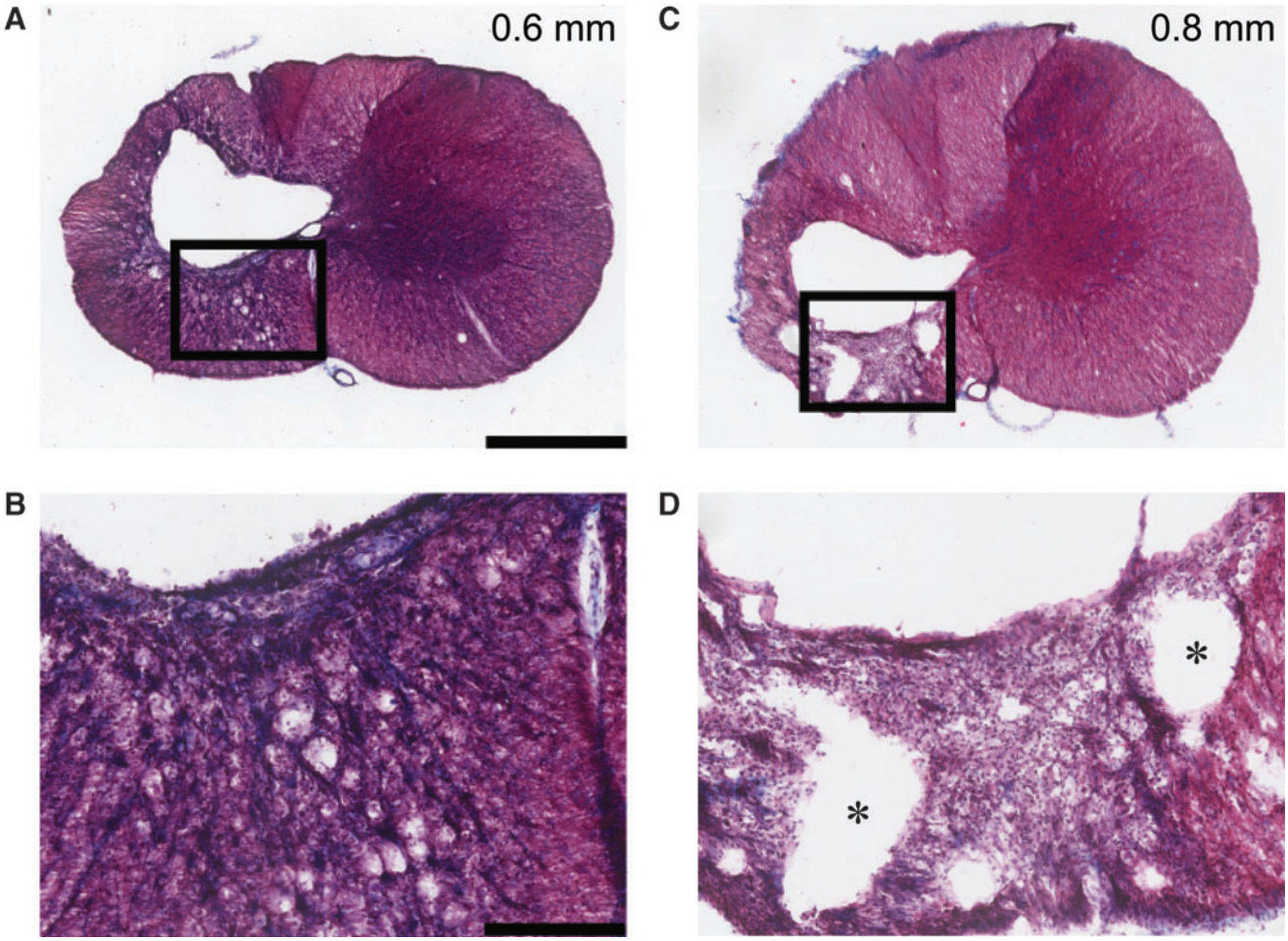

FIG. 8. Example trichrome stain of injury epicenter. Masson's trichrome stain taken from the epicenter of one representative animal from each injury group; 0.6 mm **(A,B)** and 0.8 mm **(C,D)** displacement. Black box in A, C is enlarged below in B, D to illustrate scar thickness. Note that microcysts, particularly in the ventral spinal white matter, are more apparent in the 0.8 than 0.6 mm injury. Scale bar = 1 mm (A,C), and 250 μm (B,D). Red staining = cytoplasm, blue staining = collagen (* indicate microcysts). Color image is available online at www.liebertpub.com/neu

group, who had only minor and short-lived deficits. These included measures such as swing duration, duty cycle, and swing speed in the CatWalk task, as well as predominant elbow joint position and proximal forelimb movements on the IBB task. However, deficits of the distal joint forelimb functions were pronounced in 0.6 mm displacement animals. Predominant forepaw position, cereal adjustments, wrist movement during manipulation, and paw contact during the IBB task all were significantly different from intact animals for the full 12 weeks post-injury. While previous publications on cervical contusion modeling have also shown significant differences between the different injury magnitudes on features of the CatWalk task,[8,16,23] they did not identify a group separation between the recovery of proximal versus distal features as described here. This may be a result of prior studies not assessing functional deficits on the IBB task, or result from the greater separation and more severe injuries utilized in earlier studies.

The forelimb asymmetry use task did not resolve the different injury magnitudes in this injury model. This is likely due to the fact that this test assesses the animals' preference for using either of the forelimbs independently or together and does not necessarily measure the animal's ability to use the forelimbs based on motor deficits. In addition, this lack of difference may be due to the less severe injury magnitudes used in the current study. Studies using more severe injury magnitudes reported significant differences between the light and severe injury groups when the severe injury group had more dramatic forelimb impairments.[8,23]

Myelination and rostral spread of the lesion void may predict behavioral outcomes following cervical hemi-contusion

The lack of a significant difference in spared ipsilateral gray matter, white matter, and lesion void area between injury groups, accompanied by a significant difference in ipsilateral white matter myelination between the injury groups, indicates that spared myelinated fibers may give rise to the robust behavioral separation observed between groups. Indeed, myelination is critical for the fast transduction of neural signals throughout the nervous system and a decrease in myelination has been shown to greatly impair axonal conductance after injury.[26–28] Here, we report that the more severe 0.8 mm injury group has significantly less ipsilateral white matter myelination, compared with the 0.6 mm animals, suggesting that their more exacerbated deficits result from this increased loss of myelination. Similarly, prior cervical contusion modeling studies all reported a decrease in ipsilateral white matter.[8,16,23] In these prior studies, however, differences in gray matter were only present

in those groups that differed the most in severity (e.g., 0.8 versus 1.1 displacement).[8] This suggests that the gray matter is secondarily affected in rodent contusion spinal cord injuries, compared with white matter, and primarily occurs in more severe injuries.

Regional assessments of ipsilateral white matter demyelination demonstrated that the significant decrease in myelinated white matter was primarily restricted to the lateral region of the hemicord containing the RST. Prior studies have reported this tract to be important for unrestrained overground locomotion, captured here by performance on the CatWalk.[29–31] Such findings suggest that the lack of myelinated RST in the 0.8 mm groups may have produced the more prolonged proximal forelimb deficits seen on the CatWalk and IBB tasks in comparison to the 0.6 mm group.

This same lack of myelinated lateral region of the cord also may be responsible for prolonged distal forelimb deficits reported in the 0.6 mm group. In addition to being responsible for more proximally dependent functions like the CatWalk, the RST also has been shown to play a strong role in controlling more distal forelimb functions, like pellet reaching tasks[32–35] and staircase pellet reaching tasks.[34,36] While these tasks were not assessed in the current study, the IBB task involves comparable distal forelimb functions.[18] It will be important in the future to examine fine motor function between injury severities using measures of forelimb function as we have done for this model recently.[13,14]

Although not significantly different, the myelinated area of the ventral region in the 0.8 mm group tended to be less than in the 0.6 mm group. In addition, gross observation of micro-cysts by trichrome staining corroborated the likelihood of increased axonal and myelin degeneration in this region. In turn, the reticulospinal and propriospinal tracts located in this region of the cord are known to be particularly important for locomotion and gait.[37–40] The increased damage to these tracts may also have played a role in the more prolonged deficits seen in the 0.8 mm group on the CatWalk, as well as the proximal sub-scores during the IBB task. Reticulospinal and propriospinal nerve fiber mapping may provide a better understanding of the role of these pathways in spared function.

Increased rostral spread of the injury void and demyelinated areas in the 0.8 mm group, compared with 0.6 mm group, may also contribute to the increased deficits and prolonged recovery reported in the 0.8 mm group. Axonal fibers must sprout or regenerate longer distances in order to effectively cross these regions of injury and create new circuitry capable of restoring function. This type of plasticity has been shown to occur spontaneously in the spinal cord after a T8 dorsal hemisection.[5] This bridge was reported to begin at C3, with increased supraspinal sprouting into the central gray matter. Here, we suspect a similar type of plasticity is possible, particularly the 0.6 mm group, as their injury spreads less into the C3 spinal segment, compared with the 0.8 mm group. In this regard, the cervical hemi-contusion injury model could allow for the testing of methods to enhance plasticity functional recovery after injury.

Advantages of the C4 hemi-contusion model for investigating translational cervical SCI therapeutics targeting proximal or distal upper limb recovery

The C4 hemi-contusion leads to a relatively circumscribed loss of gray matter at the site of the impact but spares circuitry in the C5 segment and below. Hence, this model likely leaves the motoneurons and interneurons responsible for hand and wrist function intact. White matter injury is more wide-spread and the amount of white matter loss correlates with injury severity. Hence, this model may be well-suited for studies aiming to increase axonal growth, plasticity or myelination of spared pathways. The model shows important similarities with human injury of a corresponding level. For example, incomplete cervical spinal cord injury leads to deficits in the control of proximal muscles important for overall arm positioning, as well as muscles important for tasks needed for self-care, eating, and writing. The ESCID C4 hemi-contusion model exhibits similar deficits of volitional control of the hand and wrist, which are likely tied to the loss of descending inputs to the spared motoneurons in caudal segments. Improvements in the proximal and distal joints are necessary to regain autonomy for those with SCI, thus treatments focused on each of these regions of the upper limb are necessary. Unfortunately, addressing both in the same model is challenging. Persistent proximal deficits present in more severe injuries, as seen in our 0.8 mm group, are typically paired with pronounced distal deficits. Here, proximal recovery is possible but distal recovery may be unrealistic, as those tasks requiring distal joint manipulation are difficult to achieve due to the lack of proximal function (i.e., lifting the arm to reach for food reward). Less severe injuries, like 0.6 mm group exhibiting transient proximal deficits but persistent distal deficits, have a much greater possibility for enhanced distal recovery. Treatments for proximal limb recovery, however, may be difficult to assess, as recovery of proximal function occurs spontaneously. Nonetheless, our finding that the C4 cervical hemi-contusion injury produced by the updated ESCID can be graded via different displacement parameters to either enable or prevent distal forelimb recovery reinforces its value as a model for testing treatments targeting the nerves critical for motor control of the forelimb.

Conclusion

The findings in the current study indicate that the updated ESCID produces consistent injuries within small groups of rats and can be used to create graded behavioral outcomes. Injuries with a displacement of 0.8 mm result in severe motor deficits that affect both proximal and distal forelimb functions and persist for at least 12 weeks following injury. The 0.6 mm displacement is a much less severe injury, only interfering primarily with distal forelimb functions for prolonged periods of time. These behavioral group differences may result from decreased myelination or axonal sparing due to the more pronounced rostrally extending lesion voids in the 0.8 mm group. Combined with observed functional deficits, the decreased amount of myelinated area in the dorso-lateral white matter implicates damage to the RST in the behavioral group differences. Overall, we conclude that the C4 cervical hemi-contusion injury model using the updated ESCID is beneficial for testing therapies aiming to enhance both proximal and distal upper limb functions, as well as those aiming to enhance lesion-bypassing plasticity.

Acknowledgments

This work was supported by an NIH EUREKA grant NS066357 (PJH, CTM), the Craig H. Neilsen Foundation (259314-CTM, 296453-SEM), Raymond and Beverly Sackler Scholars Program in Integrative Biophysics (SEM), the Center for Sensorimotor Neural Engineering (CSNE), a National Engineering Research Center (1028725), a Paul G. Allen Family Foundation Allen Distinguished Investigator Award (CTM), and a generous gift from the Irv Naylor Foundation (PJH). PJH is a member of the University of Washington Center on Human Development and Disability.

Author Disclosure Statement

No competing financial interests exist.

References

1. Sekhon, L.H. and Fehlings, M.G. (2001). Epidemiology, demographics, and pathophysiology of acute spinal cord injury. Spine 26, S2–S12.
2. Norenberg, M.D., Smith, J., and Marcillo, A. (2004). The pathology of human spinal cord injury: defining the problems. J. Neurotrauma 21, 429–440.
3. Anderson, K.D. (2004). Targeting recovery: priorities of the spinal cord-injured population. J. Neurotrauma 21, 1371–1383.
4. Raineteau, O. and Schwab, M.E. (2001). Plasticity of motor systems after incomplete spinal cord injury. Nat. Rev. Neurosci. 2, 263–273.
5. Bareyre, F.M., Kerschensteiner, M., Raineteau, O., Mettenleiter, T.C., Weinmann, O., and Schwab, M.E. (2004). The injured spinal cord spontaneously forms a new intraspinal circuit in adult rats. Nat. Neurosci. 7, 269–277.
6. Courtine, G., Song, B., Roy, R.R., Zhong, H., Herrmann, J.E., Ao, Y., Qi, J., Edgerton, V.R., and Sofroniew, M.V. (2008). Recovery of supraspinal control of stepping via indirect propriospinal relay connections after spinal cord injury. Nat. Med. 14, 69–74.
7. Stokes, B.T., Noyes, D.H., and Behrmann, D.L. (1992). An electromechanical spinal injury technique with dynamic sensitivity. J. Neurotrauma 9, 187–195.
8. Pearse, D.D., Lo, T.P., Cho, K.S., Lynch, M.P., Garg, M.S., Marcillo, A.E., Sanchez, A.R., Cruz, Y., and Dietrich, W.D. (2005). Histopathological and behavioral characterization of a novel cervical spinal cord displacement contusion injury in the rat. J. Neurotrauma 22, 680–702.
9. Bresnahan, J.C., Beattie, M.S., Todd, F.D., and Noyes, D.H. (1987). A behavioral and anatomical analysis of spinal cord injury produced by a feedback-controlled impaction device. Exp. Neurol. 95, 548–570.
10. Bresnahan, J.C., Beattie, M.S., Stokes, B.T., and Conway, K.M. (1991). Three-dimensional computer-assisted analysis of graded contusion lesions in the spinal cord of the rat. J. Neurotrauma 8, 91–101.
11. Bresnahan, J.C., Behrmann, D.L., and Beattie, M.S. (1993). Anatomical and behavioral outcome after spinal cord contusion injury produced by a displacement controlled impact device. Restor. Neurol. Neurosci. 5, 76.
12. Behrmann, D.L., Bresnahan, J.C., Beattie, M.S., and Shah, B.R. (1992). Spinal cord injury produced by consistent mechanical displacement of the cord in rats: behavioral and histologic analysis. J. Neurotrauma 9, 197–217.
13. Nutt, S.E., Chang, E.-A., Suhr, S.T., Schlosser, L.O., Mondello, S.E., Moritz, C.T., Cibelli, J.B., and Horner, P.J. (2013). Caudalized human iPSC-derived neural progenitor cells produce neurons and glia but fail to restore function in an early chronic spinal cord injury model. Exp. Neurol. 248, 491–503.
14. Kasten, M.R., Sunshine, M.D., Secrist, E.S., Horner, P.J., and Moritz, C.T. (2013). Therapeutic intraspinal microstimulation improves forelimb function after cervical contusion injury. J. Neural Eng. 10, 044001.
15. Sunshine, M.D., Cho, F.S., Lockwood, D.R., Fechko, A.S., Kasten, M.R., and Moritz, C.T. (2013). Cervical intraspinal microstimulation evokes robust forelimb movements before and after injury. J. Neural Eng. 10, 036001.
16. Dunham, K.A., Siriphorn, A., Chompoopong, S., and Floyd, C.L. (2010). Characterization of a graded cervical hemicontusion spinal cord injury model in adult male rats. J. Neurotrauma 27, 2091–2106.
17. Côté, M.P., Detloff, M.R., Wade, R.J., Lemay, M.A., and Houlé, J.D. (2012). Plasticity in ascending long propriospinal and descending supraspinal pathways in chronic cervical spinal cord injured rats. Front. Physiol. 3, 330.
18. Irvine, K.A., Ferguson, A.R., Mitchell, K.D., Beattie, S.B., Lin, A., Stuck, E.D., Huie, J.R., Nielson, J.L., Talbott, J.F., Inoue, T., Beattie, M.S., and Bresnahan, J.C. (2014). The Irvine, Beatties, and Bresnahan (IBB) forelimb recovery scale: an assessment of reliability and validity. Front. Neurol. 5, 116.
19. Irvine, K.A., Ferguson, A.R., Mitchell, K.D., Beattie, S.B., Beattie, M.S., and Bresnahan, J.C. (2010). A novel method for assessing proximal and distal forelimb function in the rat: the Irvine, Beatties and Bresnahan (IBB) forelimb scale. J. Vis. Exp. pii, 2246
20. White, B.D., Nathe, R.J., Maris, D.O., Nguyen, N.K., Goodson, J.M., Moon, R.T., and Horner, P.J. (2010). Beta-catenin signaling increases in proliferating NG2 + progenitors and astrocytes during post-traumatic gliogenesis in the adult brain. Stem Cells 28, 297–307.
21. Hamers, F.P.T., Koopmans, G.C., and Joosten, E.A.J. (2006). CatWalk-Assisted Gait Analysis in the Assessment of Spinal Cord Injury. J. Neurotrauma 23, 537–548.
22. Schallert, T., Fleming, S.M., Leasure, J.L., Tillerson, J.L., and Bland, S.T. (2000). CNS plasticity and assessment of forelimb sensorimotor outcome in unilateral rat models of stroke, cortical ablation, parkinsonism and spinal cord injury. Neuropharmacology 39, 777–787.
23. Gensel, J.C., Tovar, C.A., Hamers, F.P.T., Deibert, R.J., Beattie, M.S., and Bresnahan, J.C. (2006). Behavioral and histological characterization of unilateral cervical spinal cord contusion injury in rats. J. Neurotrauma 23, 36–54.
24. Zhou, H., Huang, C., Chen, H., Wang, D., Landel, C.P., Xia, P.Y., Bowser, R., Liu, Y.J., and Xia, X.G. (2010). Transgenic Rat Model of Neurodegeneration Caused by Mutation in the TDP Gene. PLoS Genet 6, e1000887.
25. Beattie, M.S. (1992). Anatomic and behavioral outcome after spinal cord injury produced by a displacement controlled impact device. J. Neurotrauma 9, 157–159.
26. Blight, A.R. (1983). Cellular morphology of chronic spinal cord injury in the cat: analysis of myelinated axons by line-sampling. Neuroscience 10, 521–543.
27. Blight, A.R. (1983). Axonal physiology of chronic spinal cord injury in the cat: Intracellular recording in vitro. Neuroscience 10, 1471–1486.
28. Plemel, J.R., Keough, M.B., Duncan, G.J., Sparling, J.S., Yong, V.W., Stys, P.K., and Tetzlaff, W. (2014). Remyelination after spinal cord injury: is it a target for repair? Prog. Neurobiol. 117, 54–72.
29. Rho, M.J., Lavoie, S., and Drew, T. (1999). Effects of red nucleus microstimulation on the locomotor pattern and timing in the intact cat: a comparison with the motor cortex. J. Neurophysiol. 81, 2297–2315.
30. Muir, G.D. and Whishaw, I.Q. (2000). Red nucleus lesions impair overground locomotion in rats: a kinetic analysis. Eur. J. Neurosci. 12, 1113–1122.
31. Webb, A.A. and Muir, G.D. (2003). Unilateral dorsal column and rubrospinal tract injuries affect overground locomotion in the unrestrained rat. Eur. J. Neurosci. 18, 412–422.
32. Schrimsher, G.W. and Reier, P.J. (1993). Forelimb motor performance following dorsal column, dorsolateral funiculi, or ventrolateral funiculi lesions of the cervical spinal cord in the rat. Exp. Neurol. 120, 264–276.
33. Anderson, K.D., Gunawan, A., and Steward, O. (2007). Spinal pathways involved in the control of forelimb motor function in rats. Exp. Neurol. 206, 318–331.
34. Stackhouse, S.K., Murray, M., and Shumsky, J.S. (2008). Effect of cervical dorsolateral funiculotomy on reach-to-grasp function in the rat. J. Neurotrauma 25, 1039–1047.
35. Morris, R., Tosolini, A.P., Goldstein, J.D., and Whishaw, I.Q. (2011). Impaired arpeggio movement in skilled reaching by rubrospinal tract lesions in the rat: a behavioral/anatomical fractionation. J. Neurotrauma 28, 2439–2451.
36. Hilton, B.J., Assinck, P., Duncan, G.J., Lu, D., Lo, S., and Tetzlaff, W. (2013). Dorsolateral funiculus lesioning of the mouse cervical spinal cord at C4 but not at C6 results in sustained forelimb motor deficits. J. Neurotrauma 30, 1070–1083.
37. Grillner, S., and Zangger, P. (1979). On the central generation of locomotion in the low spinal cat. Exp. Brain Res. 34, 241–261.
38. Eidelberg, E., Story, J.L., Walden, J.G., and Meyer, B.L. (1981). Anatomical correlates of return of locomotor function after partial spinal cord lesions in cats. Exp. Brain Res. 42, 81–88.
39. Jell, R.M., Elliott, C., and Jordan, L.M. (1985). Initiation of locomotion from the mesencephalic locomotor region: effects of selective brainstem lesions. Brain Res. 328, 121–128.
40. Schepens, B., Stapley, P., and Drew, T. (2008). Neurons in the pontomedullary reticular formation signal posture and movement both as an integrated behavior and independently. J. Neurophysiol. 100, 2235–2253.

Address correspondence to:
Philip J. Horner, PhD
Houston Methodist Research Institute
Center for Neuroregenerative Medicine
4470 Bertner Avenue, MSR-10-112
Houston, TX 77030

E-mail: pjhorner@houstonmethodist.org